Annual Report • November 1991

HIGH-SPEED, HIGH-DENSITY, COHERENT TIME DOMAIN OPTICAL MEMORY

Prepared by:

Ravinder Kachru, Senior Research Physicist
Xiao-An Shen, Postdoctoral Fellow
Molecular Physics Laboratory

SRI Project PYU 1563
Contract No. F-49620-90-C-0083
MP 91-239

Prepared for:

Air Force Office of Scientific Research
Building 410
Bolling Air Force Base, DC 20332-6448

Attn: Dr. Alan Craig

HIGH-SPEED, HIGH-DENSITY, COHERENT TIME DOMAIN OPTICAL MEMORY

Prepared by:

Ravinder Kachru, Senior Research Physicist
Xiao-An Shen, Postdoctoral Fellow
Molecular Physics Laboratory

SRI Project PYU 1563
Contract No. F-49620-90-C-0083
MP 91-239

Prepared for:

Air Force Office of Scientific Research
Building 410
Bolling Air Force Base, DC 20332-6448

Attn: Dr. Alan Craig

Approved:

Donald J. Eckstrom, Director
Molecular Physics Laboratory

David M. Golden
Vice President
Physical Sciences Division

SRI International 333 Ravenswood Avenue • Menlo Park, CA 94025-3493 • (415) 326-6200 • FAX (415) 326-5512 • Telex 334486

REPORT DOCUMENTATION PAGE

Form Approved OMB No. 0704-0188

1. AGENCY USE ONLY *(Leave blank)*	2. REPORT DATE	3. REPORT TYPE AND DATES COVERED
	November 1991	Annual Report

4. TITLE AND SUBTITLE
High-Speed, High-Density, Coherent Time Domain Optical Memory

5. FUNDING NUMBERS
C:F-49620-90-C-0083

6. AUTHOR(S)
R. Kachru and X-A. Shen

7. PERFORMING ORGANIZATION NAME(S) AND ADDRESS(ES)
SRI International
333 Ravenswood Avenue
Menlo Park, CA 94025

8. PERFORMING ORGANIZATION REPORT NUMBER
MP 91-239

9. SPONSORING/MONITORING AGENCY NAME(S) AND ADDRESS(ES)
Air Force Office of Scientific Research
Building 410
Bolling Air Force Base, DC 20332-6448
Alan Craig

10. SPONSORING/MONITORING AGENCY REPORT NUMBER
2305/B4

11. SUPPLEMENTARY NOTES

12a. DISTRIBUTION/AVAILABILITY STATEMENT
Approved for public release; Distribution unlimited

12b. DISTRIBUTION CODE

13. ABSTRACT *(Maximum 200 words)*

Our goal is to quantitatively evaluate the concept of time-domain optical memory (TDOM) based on the stimulated photon echo technique and to prepare for the development of a working prototype. Earlier feasibility studies at SRI International showed that TDOM can store not only digital data in the form of a series of on-off laser pulses but also two-dimensional (2-D) images with the same read/write speed. Despite work at SRI and elsewhere, until now the use of TDOM for 2-D images has not been carefully examined and the quality of echo images and their inherent spatial resolution have not been explored. These issues have an important bearing on TDOM as a high-speed, high-density storage device.

This year, we focused on using the stimulated echo technique for 2-D image storage and image processing. Specific tasks included incorporating a gated intensified charge-coupled device (CCD) camera system for detecting echo images, digitally recording the echo images, and optimizing the optical system. We have also extended the earlier feasibility study on stimulated-echo-based, 2-D image storage and image processing and demonstrated storage and retrieval of the high-quality, high-resolution echo images. In addition, we demonstrated for the first time that nanosecond pattern recognition can be achieved using the stimulated echo approach.

14. SUBJECT TERMS	15. NUMBER OF PAGES
Stimulated photon echoes, optical memory, image processing, pattern recognition, phase conjugation	40
	16. PRICE CODE

17. SECURITY CLASSIFICATION OF REPORT	18. SECURITY CLASSIFICATION OF THIS PAGE	19. SECURITY CLASSIFICATION OF ABSTRACT	20. LIMITATION OF ABSTRACT
Unclassified	Unclassified	Unclassified	UL

PREFACE

This annual report describes progress on the research sponsored by the Air Force Office of Scientific Research under Contract Number F49620-90-C-0083. The interest and support of Project Monitor, Dr. Alan Craig, are sincerely acknowledged.

The authors are grateful to the following individuals for their help with this work: scientific discussions with Dr. Yu Sheng Bai and Dr. David Huestis were very helpful to the authors; technical assistance by various staff members at SRI is also acknowledged.

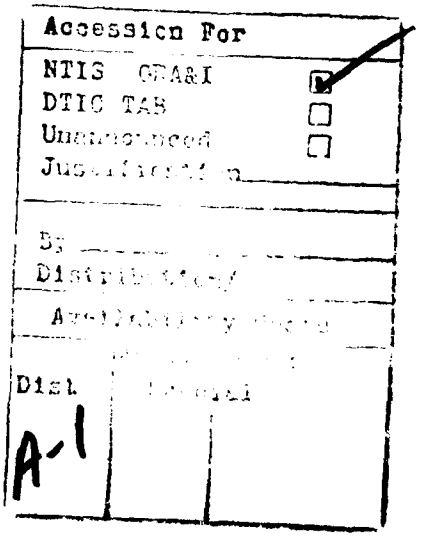

CONTENTS

INTRODUCTION

The objective of this project is to make an in-depth evaluation of the concept of time-domain optical memory (TDOM)—a new memory scheme based on stimulated photon echoes. Such a memory scheme would provide a high-speed, high-density, all-optics means for data storage. In the proposal for this project,[1] we estimated that a potential storage density of 10^5 bits/spot (approximately 10^{-6} cm^2) and a write/read rate of 10^{11} bits/s can be achieved using the stimulated echo approach. Thus, improvements of several orders of magnitude over existing memory devices would be expected.

The above estimates of density and speed were based on the concept of storing digital data encoded by a laser pulse train representing a series of digital 1's (presence of a laser pulse) and 0's (absence of a laser pulse). However, these two estimated values can be increased substantially if the data pulses carry additional spatial information, namely, 2-dimensional (2-D) images. This parallel storage approach using 2-D images has been demonstrated recently,[2,3] and the results showed no measurable effect on the write speed. Thus, a potential high-speed, high-density, page-oriented, all-optics memory is possible with the stimulated photon echo.

However, the quality of the retrieved images in the earlier demonstration[2,3] of stimulated echo image storage was generally very poor. No attempt was made to address issues regarding their intrinsic spatial resolution, the fidelity of the retrieved images, and the likely causes of various image distortions, for example. However, these issues are vital in evaluating TDOM. Our first-year effort, under AFOSR Contract No. F49620-90-C-0083, focused on addressing these issues. Our objectives were to examine the quality of echo images under various experimental conditions by recording them with precision and to explore the significance of the results with regard to the future development of a working prototype.

With the above objectives in mind, we first developed a new experimental method that permits us to make accurate, time-resolved recordings of echo images. The work involved incorporation of a gated intensified (CCD) camera and digital recording of echo images with a frame grabber. The recording system to a large degree met all of our requirements and allowed us to make quantitative evaluations of echo images.

In the next stage of the work, we performed a number of experiments related to stimulated echo image storage and image processing. The material used in these experiments was Pr^{3+}:LaF_3. We chose this material because it has a relatively short storage time[4] and experiments could be

performed at a high repetition rate (i.e., 10 Hz). We further demonstrated the possibility of performing nanosecond pattern recognition using the stimulated echo. This report summarizes the results and findings obtained from these experiments. They will be analyzed and discussed in more detail in forthcoming publications.

BACKGROUND AND APPROACH

This section briefly describes how stimulated photon echoes can be used as a means for ultrafast, high-density, image storage and then discusses an experimental arrangement we used for storing, retrieving, and processing images. A detailed discussion of the physical basis of stimulated photon echoes can be found elsewhere.[5-7]

THE STIMULATED PHOTON ECHO AS A MEANS FOR DATA STORAGE

For simplicity, consider storing only one data pulse in a rare-earth solid, e.g., Pr^{3+}:LaF_3. The analysis here can be easily generalized to cases where multiple data pulses are used. To further simplify the discussion, the excitation pulses are assumed to be monochromatic, with a frequency ω_0 that corresponds to the center of an inhomogeneously broadened absorption line of interest. The propagation directions and the temporal sequence of the excitation pulses are shown in Figure 1.

Upon interaction of the first pulse (i.e., the data pulse) with the crystal at t_1, a fraction of the rare-earth ions are excited from their ground state to the excited state. Because of the coherent nature of the data pulse, the dipoles of all the excited ions have the same phase (determined by the excitation electric field) but oscillate at their own frequency ω, which differs slightly from the laser frequency because of inhomogeneous broadening. When the write pulse arrives at the sample at t_2, some of the dipoles excited by the data pulse may not be in phase with the write pulse because of the difference in the oscillation frequency. This interference (or phase difference) between the write pulse and the electric dipole moment of all the excited ions results in population modulation in both the ground state and the excited state as a function of the detuning frequency (the difference between oscillation frequency of a particular ion and laser frequency). Thus, the temporal history of the excitation pulses is imprinted as a modulation in the ground- and excited-state population distribution.[5]

At a later time t_3, the excited ions may relax to their ground state via either radiative or nonradiative channels, but the temporal information of the data pulse can still be retained because of the presence of the ground-state hyperfine structures.[5] The excited ions are most likely to relax to hyperfine sublevels that differ from the one where the excitation was originated. A storage time of up to several hours has been demonstrated in crystals such as Eu:$YA\ell O_3$.[8]

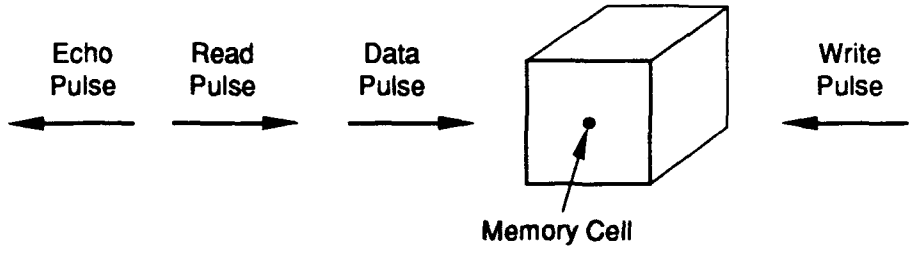

(a) Propagation direction for the data, write, and read pulses

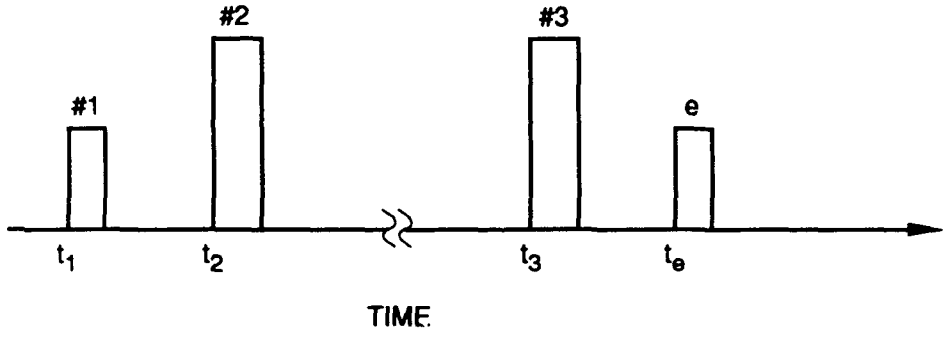

(b) Temporal sequence of the input laser pulses and echo (e) pulse.

CM-1563-4

Figure 1. Backward stimulated echo memory scheme.

When the sample is re-excited by the read pulse at t_3, the ions that underwent absorption and emission of a photon during the previous two excitations are less likely to absorb light because they are at different sublevels. As a result, the spectrally modulated ground-state distribution is converted back to temporal modulation by the read pulse, and emits an echo pulse (e), a burst of photons that is a phase-conjugate replica of the original data pulse.

As we have stated earlier, this analysis can be easily extended to multiple data pulses. However, caution must be taken to eliminate crosstalk between pulses. This can be achieved by choosing appropriate energies for data pulses. Good discussions on the subject of multiple data pulse storage can be found in Refs. 9 and 10.

EXPERIMENTAL APPARATUS

The experimental apparatus described here was developed to perform single-image storage and two-image processing. The physical basis for image processing using stimulated echoes is discussed below in the section entitled Nanosecond Image Processing. A simple modification to the system will permit the storage of multiple images (or data pulses) but is not discussed in this report.

The system (a general schematic is shown in Figure 2) consisted of a Nd:YAG pumped, pulsed dye laser operating at 477.8-nm and a gated intensified CCD camera for recording echo images. As discussed below, the 477.8 nm wavelength was chosen to coincide with the energy of the $^3P_0$ - $^3H_4$ transition in Pr^{3+}:LaF_3,[11] the material used as a storage medium in this research.

The laser pulse, approximately 5 ns long, was split into three parts by using beam splitters, two of which were optically delayed using a White Cell delay line (the optical delay line shown in Figure 2). A spatial filter was used before the beam splitters to improve the spatial profile of the laser pulses. The laser beams were expanded and collimated using beam expanders and focused onto the sample in a nearly coaxial configuration, as shown in Figure 2. Transmission masks were placed at the front focal plane of each focusing lens to obtain exact Fourier transforms of the images at the sample located at the back focal plane of the lenses. The focal length of the transform lenses was 400 mm. The echo signal emitted in the direction opposite to the first (data) pulse as a result of the phase-matching requirement was collected by the CCD camera with the aid of a beam splitter. The angle between the first and second pulses was approximately 2 degrees.

The CCD camera was gated with a 50-ns pulse and synchronized with the pulsed dye laser to allow the recording of only echo images. The sample in which the images were recorded, Pr^{3+}:LaF_3, was chosen for the investigation because it provided a relatively short storage time and thus permitted us to run our experiments at a high repetition rate for convenience. The repetition rate used in these experiments was 10 Hz.

We chose Figure 2 for our discussion of the apparatus because the schematic shown is more general and can be used for a number of applications, e.g., image storage, image processing, and pattern recognition. This setup can be modified slightly to meet the requirements of specific experiments of interest. We will discuss these modifications in the next three sections.

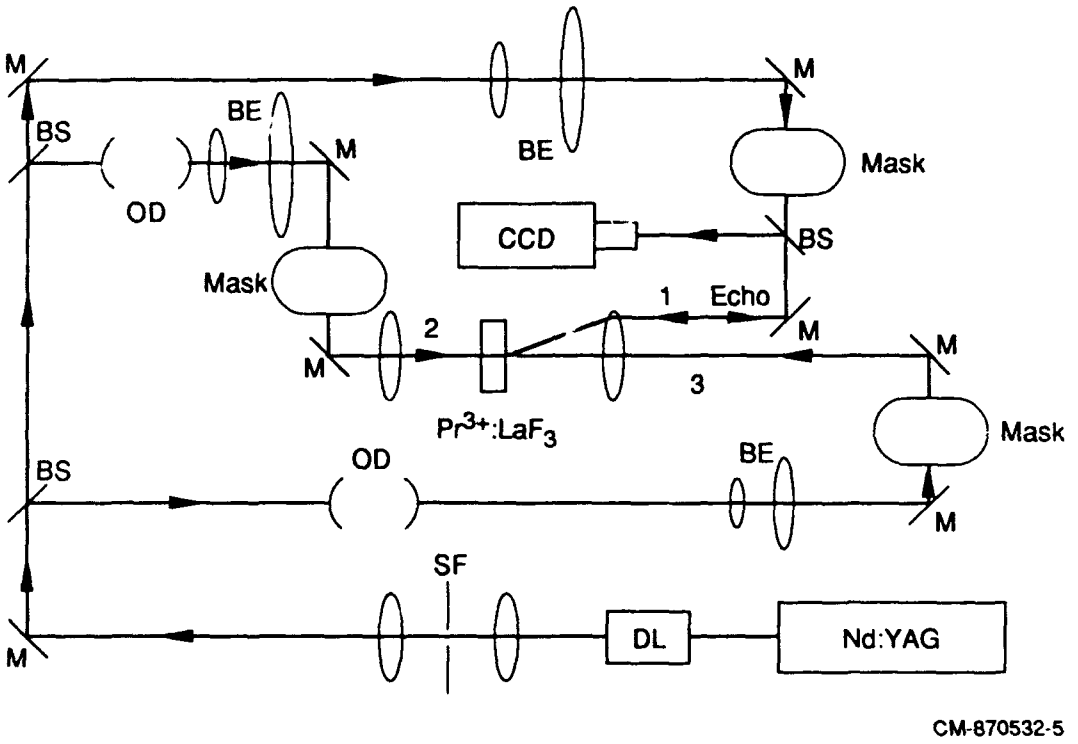

Figure 2. Schematic of the experimental apparatus for image storage and image processing using the stimulated echo technique.

BS = beam splitter; BE = beam expander; M = mirror; DL = dye laser; OD = optical delay line; CCD = intensified CCD camera; SF = spatial filter.

HIGH-SPEED IMAGE STORAGE AND RETRIEVAL

As discussed previously, our first year's work focused on examining the use of stimulated echoes for 2-D image storage and their potential use for image processing and pattern recognition. In this section, we discuss only image storage and retrieval and present some results relevant to the work. The results related to image processing and pattern recognition are presented in the next two sections.

SPATIAL IMAGE STORAGE AND RETRIEVAL

The discussion in the preceding section can be easily applied to the case of storing a 2-D image. By putting an object mask in the path of the data pulse, as shown in Figure 2, one can spatially modulate the intensity of the pulse to produce an image. If the write and read pulses are spatially uniform at the sample, then the retrieved (echo) pulse, as discussed, will be a replica of the data pulse, i.e., it will also be spatially modulated. To produce spatially uniform write and read pulses, we can either use delta function masks for the two beams, as shown in Figure 2, or remove the beam expanders and masks and insert appropriate lenses to collimate the beams at the sample. The results presented in this section were obtained using the latter approach.

In either case, the data pulse that contains an image is focused at the sample, generating a Fourier transform of the image.[12] Since the echo image propagates in the direction opposite to the data pulse, it will be transformed back by the same lens, and as a result, one will obtain an image identical to the data image. Mathematically, the amplitude of the electric field of the echo pulse is given by

$$E_e(x,y) \propto F\{\mathfrak{u}_1^*(x,y,)\}=u_1^*(x,y) \qquad (1)$$

where u_1 is the amplitude of the electric field of the data pulse, $F\{f\}$ is the spatial Fourier transform of an arbitrary function f, and $\mathfrak{u}_1$ is the spatial Fourier transform of u_1.

Since our objective was to examine use of the stimulated echo for storage of 2-D images, we first selected a Newport resolution target as a mask and recorded its echo image to examine the fidelity of the retrieved image as well as its spatial resolution. The relative delays between the first and second and between the second and third pulses were chosen to be 90 ns and 20 ns, respectively.

Figure 3 shows a retrieved image of the Newport resolution target from the stimulated echo memory. This picture was recorded from a single echo pulse by the CCD camera and digitized by the frame grabber; no averaging was performed. It is clear from Figure 3 that the quality of the retrieved image is excellent. In addition, the picture shows that closest line pairs (lp) that can be resolved in the measurement is 3.17 lp/mm (i.e., Group 1, Element 5). This limit of 3.17 lp/mm does not, however, represent the intrinsic resolution of the stimulated echo memory for spatial image storage. It only reflects the limit of our recording system (i.e., the CCD camera) in resolving fine details that are on the order of 3.17 lp/mm and higher. To prove it, we compared Figure 3 to Figure 4, a picture of the same resolution target taken by the same CCD camera, where the target was illuminated directly by a 477.8-nm laser pulse; we see no significant improvement in picture quality over the echo image.

We believe that this limit in the spatial resolution is largely due to the blooming effect caused by the microchannel-plate image intensifier in the CCD camera. This effect depends strongly on the intensity of the incident light. Although the energy of the echo pulse was very weak (on the order of 1 nJ), its temporal width was only 5 ns, which results in an echo pulse as high as several watts, powerful enough to cause a blooming effect in the intensifier.

The phase-conjugate nature of the echo pulses (see Eq. 1) in the present arrangement ensures high quality echo images because any distortion to the data images introduced by optics will be self-corrected when the images are retrieved at a later time. This finding suggests that possible distortions caused by optics can be minimized by using the first pulse in the stimulated echo to carry spatial information for image storage. We have examined using the second pulse as a data pulse and found a measurable difference in image quality.

Figure 5 shows additional examples of the images retrieved from the Pr^{3+}:LaF_3, and again the picture quality is excellent. We should point out that these experiments used black and white films as object masks except for the resolution target, which was made of an optical glass substrate with clear lines on an opaque chrome background. All the experiments were performed at temperatures between 3.6 K and 5.5 K by putting the sample in a liquid helium dewar, and a typical laser power for each pulse was around 30 μJ.

One issue that has not yet been addressed is the possible effect of temperature on the quality of the retrieved images. However, this issue is important in terms of the parallel storage scheme. We will examine this effect in the near future.

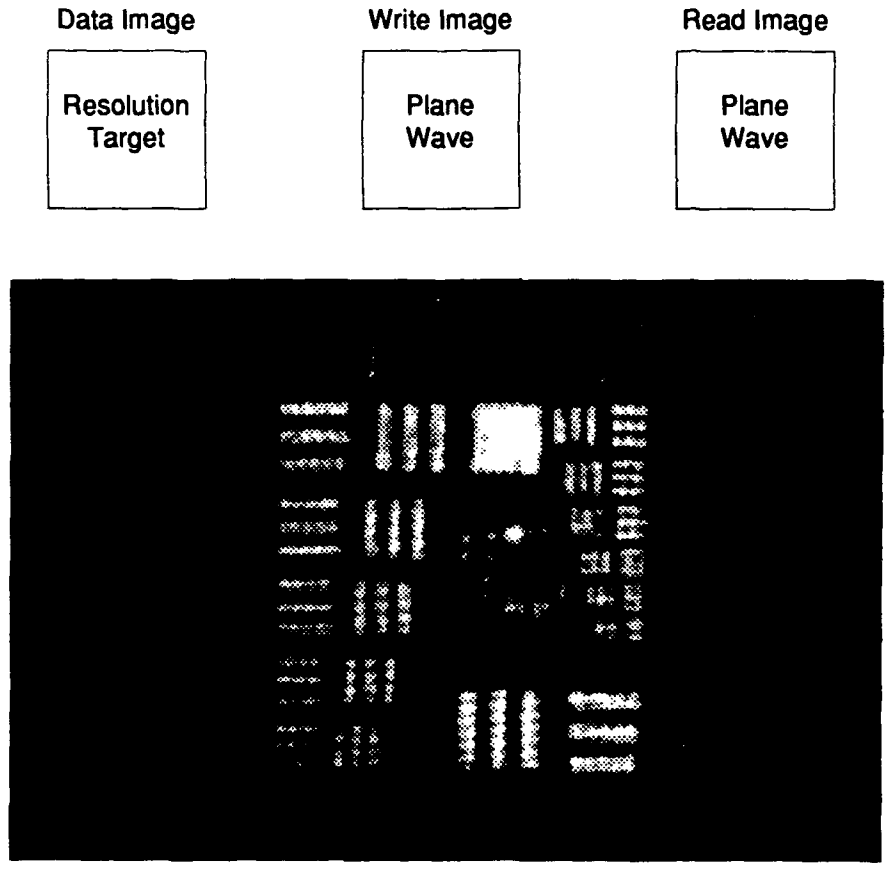

Figure 3. A photograph of the Newport resolution target retrieved from the stimulated echo memory.

The write and read pulses are plane waves.

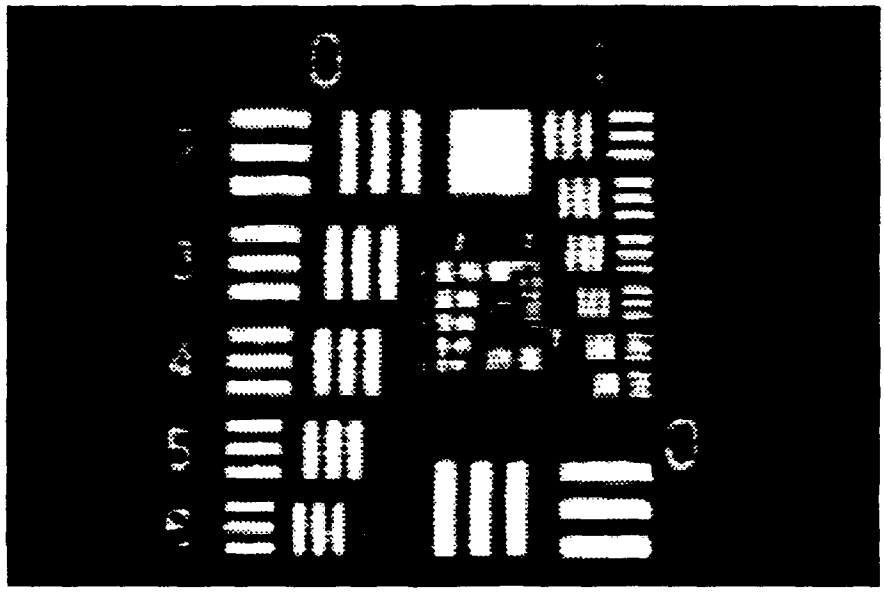

CP-1563-7

Figure 4. A photograph of the Newport resolution target illuminated with a 5-ns laser pulse at 477.8 nm.

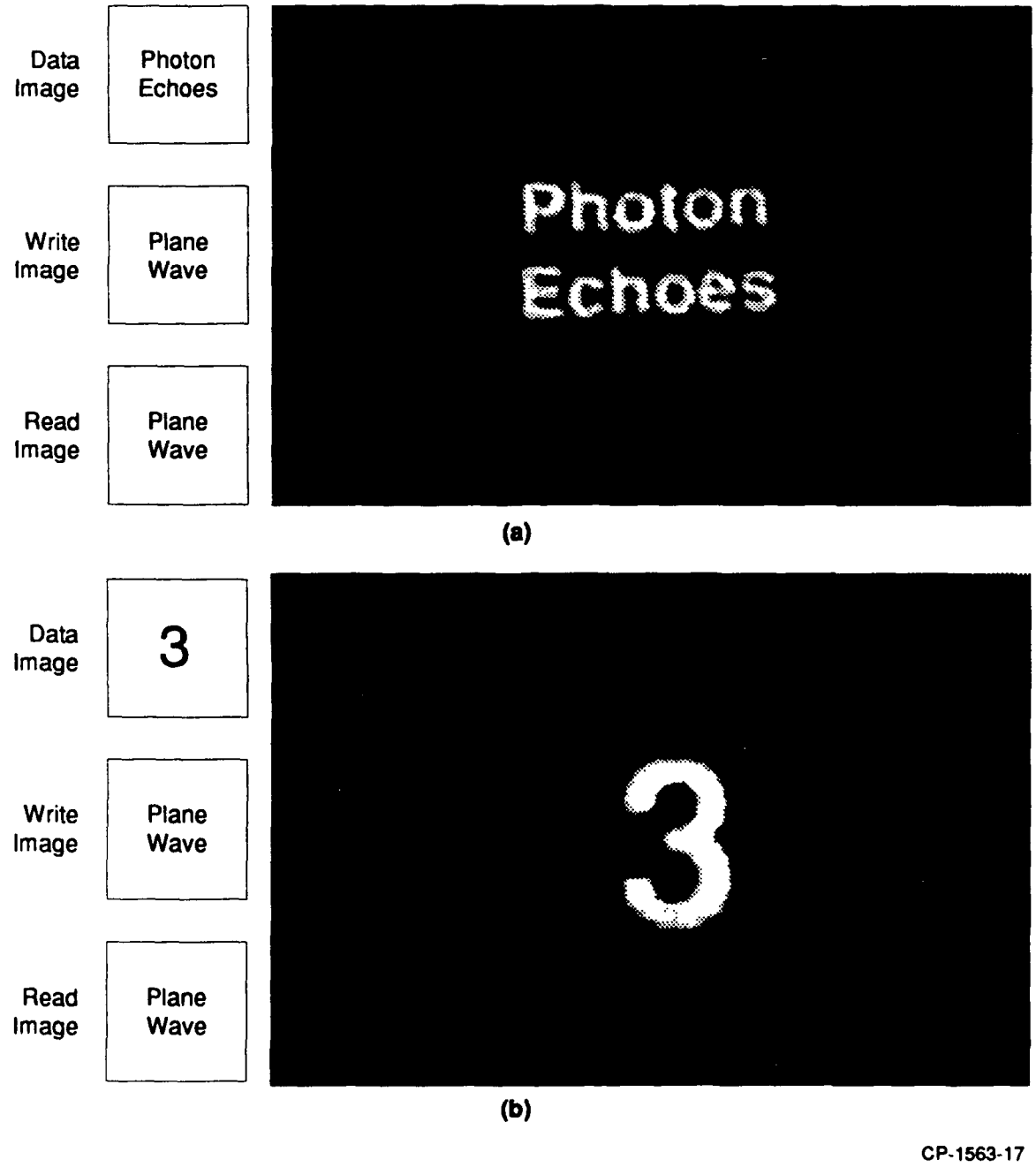

Figure 5. Additional images retrieved from the stimulated echo memory.

The above results allow us to estimate the write/read rate of our system. The typical dimensions of our data image here were 10×10 mm, with a resolution of approximately 3 lp/mm, i.e., 6 bits/mm. Thus, each data pulse contained 3600 bits. The data and write pulses, or read and echo pulses, were separated by 90 ns, which implies a write/read rate of approximately 4×10^{10} bits/s. We should point out that the estimate here is merely an example to show the already achieved write/read speed in our experiments. It is conceivable that a much higher input/output rate (several orders of magnitude larger) can be obtained with TDOM.

IMAGE STORAGE AND RETRIEVAL THROUGH AN OPTICAL FIBER

The phase-conjugate nature of the echo images opens the possibility of using fiberoptics for image input and output. In this section, we discuss the storage and retrieval of 2-D images through an optical fiber.

It is well known that image information, encoded as a spatial intensity pattern, is rapidly scrambled as it propagates in an optical fiber because of mode coupling.[13] Thus, optical fibers are often not used for image transmission. However, under certain conditions, the transmission of images can be achieved with optical fibers. One approach is to use a phase-conjugating mirror at the output of the fiber and retransmit the image through an identical fiber link. With this technique, one can remove the phase distortions of each mode and restore its original pictorial field. This idea of restoring images from optical fibers was proposed by Yariv[14] in the 1970s and has been demonstrated using standard four-wave mixing.[15,16] However, to our knowledge, no attempts have been made to explore the use of fibers for transmitting images to and from a stimulated echo storage device.

As discussed above, the retrieved image from the stimulated echo memory is a phase-conjugate replica of the data image. Thus, one can use a multimode optical fiber to deliver a data image to the stimulated echo storage medium. Even though the data image is completely scrambled after it arrives at the medium, the echo image will be restored to its original undistorted form by the fiber because it propagates back through the same link that creates the distortions.

Figure 6 shows an experimental setup used to demonstrate a fiberoptics-based stimulated echo memory. A standard single-fiber, double-pass configuration was employed for storing and retrieving images. Here the fiber was a 400-μm-diameter, 1-foot-long, multimode fiber purchased from Mitsubishi Cable America, Inc. The data image was focused into the optical fiber by a lens with 100 mm focal length, and the output was imaged onto the sample as shown in the figure. We have tested several object masks, including the Newport resolution target. The data images, as expected, were completely scrambled by the optical fiber and showed only a round spot at the

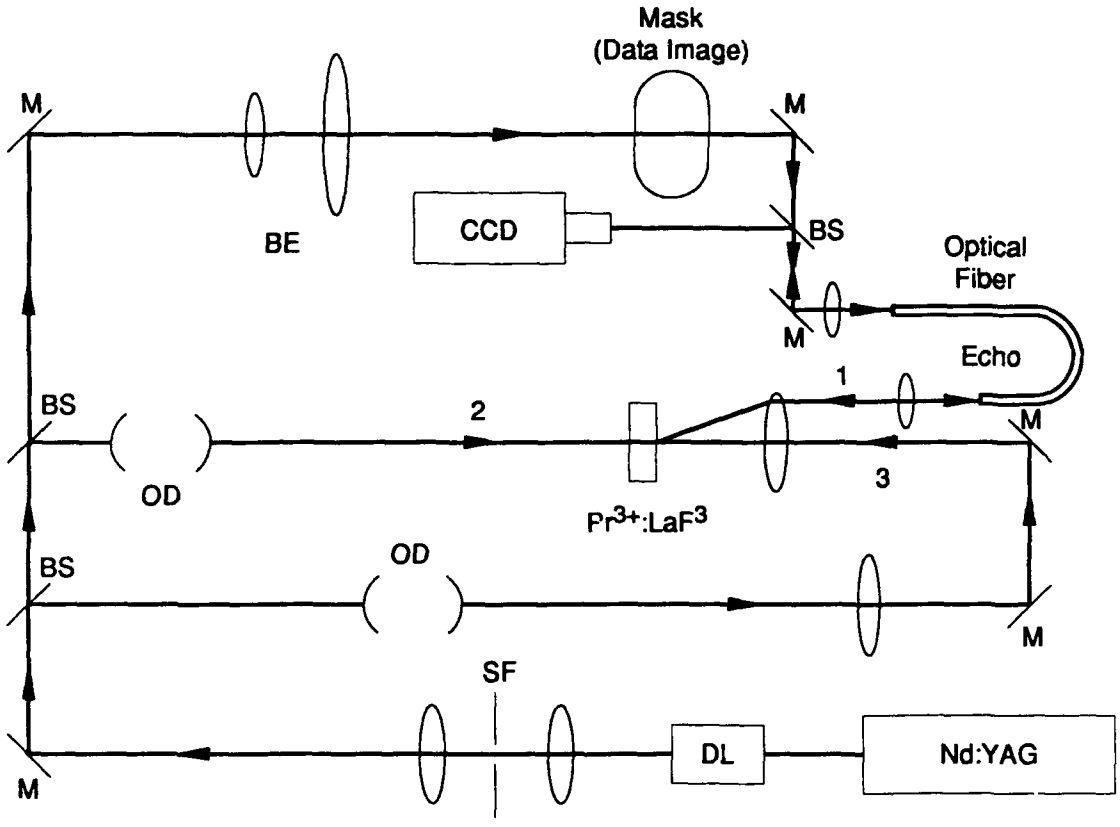

Figure 6. Experimental setup to demonstrate the phase-conjugate nature of the echo images.

BS = beam splitter; OD = optical delay; BE = beam expander; M = mirror; DL = dye laser; CCD = intensified CCD camera; SF = spatial filter.

fiber output that does not resemble at all the input images (see Figures 7b, 8b, and 9b). However, after the scrambled images were stored in the sample and later retrieved by a read pulse, the original undistorted images emerged and were recorded by the CCD camera as shown in Figures 7a, 8a, and 9a. Except for the presence of weak, scattered light from the fiber, the quality of the images retrieved through the fiber is very good; no distortion of any kind was observed.

The above results represent the first experimental evidence that optical fibers can be used in a stimulated echo memory for image input and output. This finding has a number of important implications for the future development of a prototype memory device. The memory device can be more compact with optical fibers. It will also be easy to use and require no optical alignment. In addition, multiple fibers can be employed for simultaneous storage and retrieval of a large number of images to increase the input/output rate or for storage of large images that lens systems cannot handle. Another potential application of this fiber-based optical memory would be a multi-user central memory system. Each user's data could be stored through an optical fiber in one memory location of the central system. This approach would significantly reduce the cost as well as the effort of keeping the storage medium at the required low temperatures.

These results clearly demonstrate the ability of the stimulated echo to perform high-speed image storage. The incorporation of fiberoptics open further possibilities for new applications and will have many important technological implications. The work here represents a good start toward development of a working prototype memory device. However, a number of issues need to be addressed and additional experiments are required, e.g., to find a more suitable crystal for an image storage medium, to investigate in more detail the effect of temperature on the stored images (our preliminary work on the effect of temperature is discussed later in this report), and to further improve the quality of retrieved images.

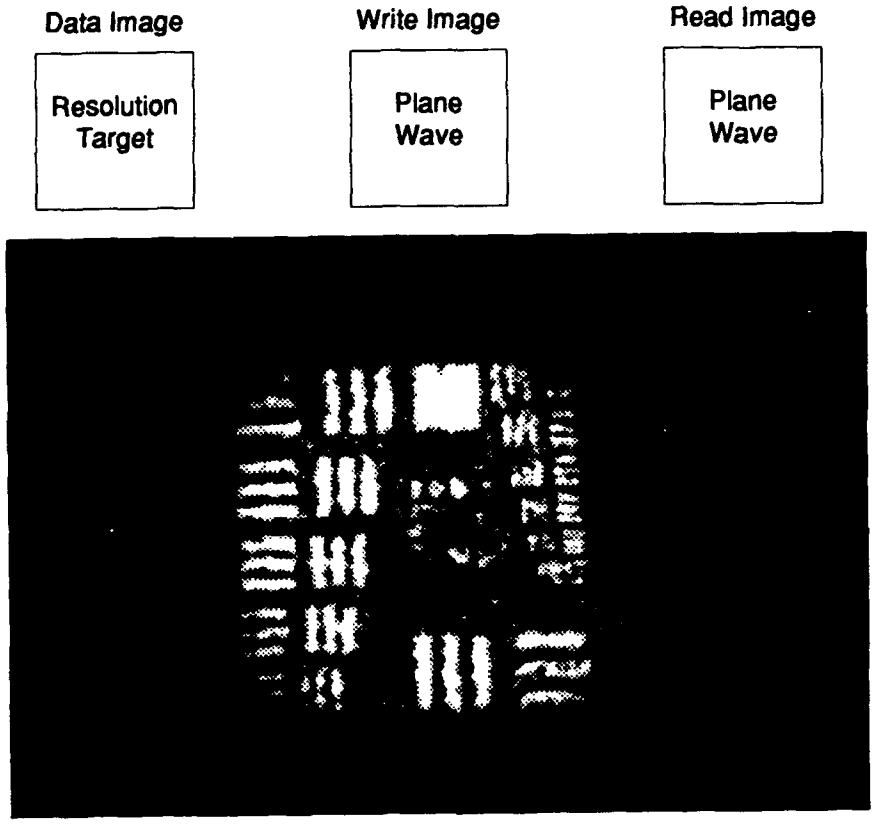

(a) Echo image retrieved through a multimode optical fiber

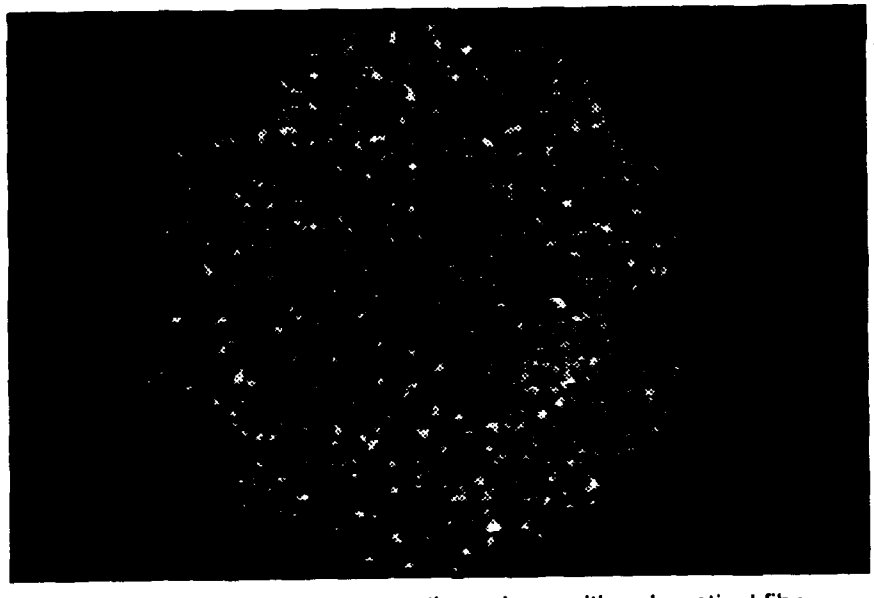

(b) Input image after passage through a multimode optical fiber

CP-1563-18

Figure 7. Photographs demonstrating the phase-conjugate nature of an echc image.

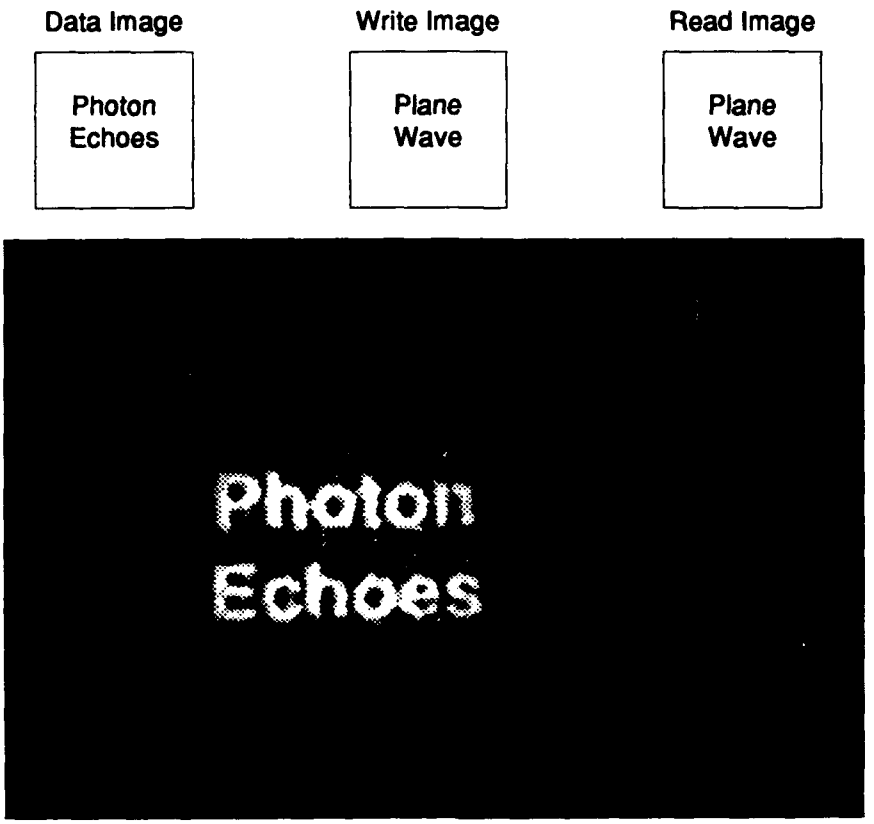

(a) Echo image retrieved through a multimode optical fiber

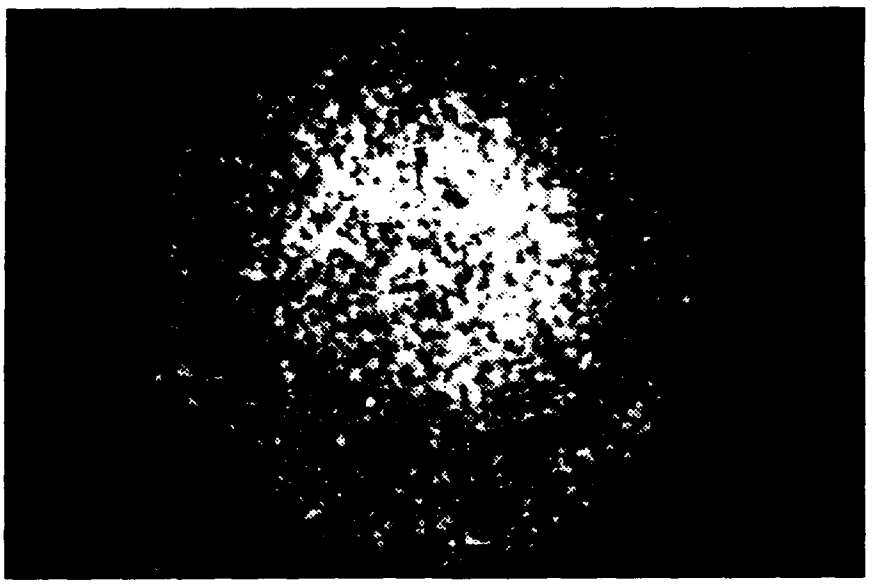

(b) Input image after passage through a multimode optical fiber

CP-1563-19

Figure 8. Photographs demonstrating the phase-conjugate nature of an echo image.

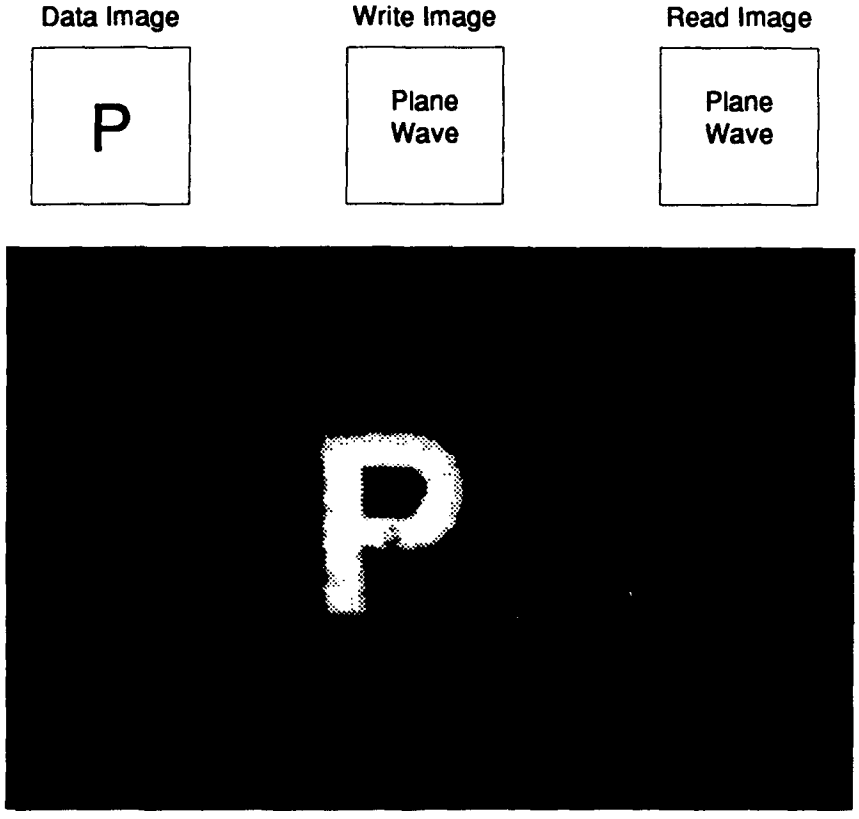

(a) Echo image retrieved through a multimode optical fiber

(b) Input image after passage through a multimode optical fiber

CP-1563-9

Figure 9. Photographs demonstrating the phase-conjugate nature of an echo image.

NANOSECOND IMAGE PROCESSING

SPATIAL CONVOLUTION AND CORRELATION

In the work described in the previous section, the write and read pulses carried no spatial information, i.e., they were plane waves. The echo image was thus a phase-conjugate replica of the data image (the first pulse). However, if the second (write) and third (read) pulses are also spatially modulated with masks and are focused into the sample as was done with the data pulse, the echo image will be a function of all three input pulses. In fact, it can be shown[17] that the echo electric field is related to the three pulses through the following equation,

$$E_e \propto u_3(-x,-y) * u_2(-x,-y) \otimes u_1(-x,-y) \qquad (2)$$

where u_i is the amplitude modulation function of the electric field of the ith pulse, and * and $\otimes$ represent spatial convolution and correlation, respectively.

The above expression states that if u_3 (or u_2) is a delta function (i.e., a plane wave at the sample), then the echo image is the correlation of u_2 (or u_3) with u_1. However, if u_1 is a delta function, the echo image is then the convolution of u_2 and u_3. Note that the above operations are performed on the inverted input images. It will be shown below that the correlation operations can be reduced to simple convolutions by choosing the appropriate form for u_1.

We have performed several experiments to demonstrate the ability of the stimulated echo to perform convolution and correlation of two images. The experimental conditions under which the measurements were conducted were identical to those in the previous section: the sample was Pr^{3+}:LaF_3; the temperature was around 4 K; and t_{12} (the delay between the first and second pulses) and t_{23} (that between the second and third pulses) were 90 ns and 20 ns, respectively. The masks used in the experiments were a numeral "5", a numeral "7", and a picture of three dots. Again, one of the three input pulses was a plane wave carrying no spatial information. Four different combinations of the masks were used; the echo images are shown in Figures 10 through 13.

As expected, the correlation operations are not symmetric with respect to change of the order of the input images (compare Figures 10 and 11), while the convolutions are (Figures 12 and 13). When u_1 is a delta function, the echo image is the convolution of the two inverted input images as stated in Eq. (2). However, when either u_2 or u_3 is a delta function, the resulting echo

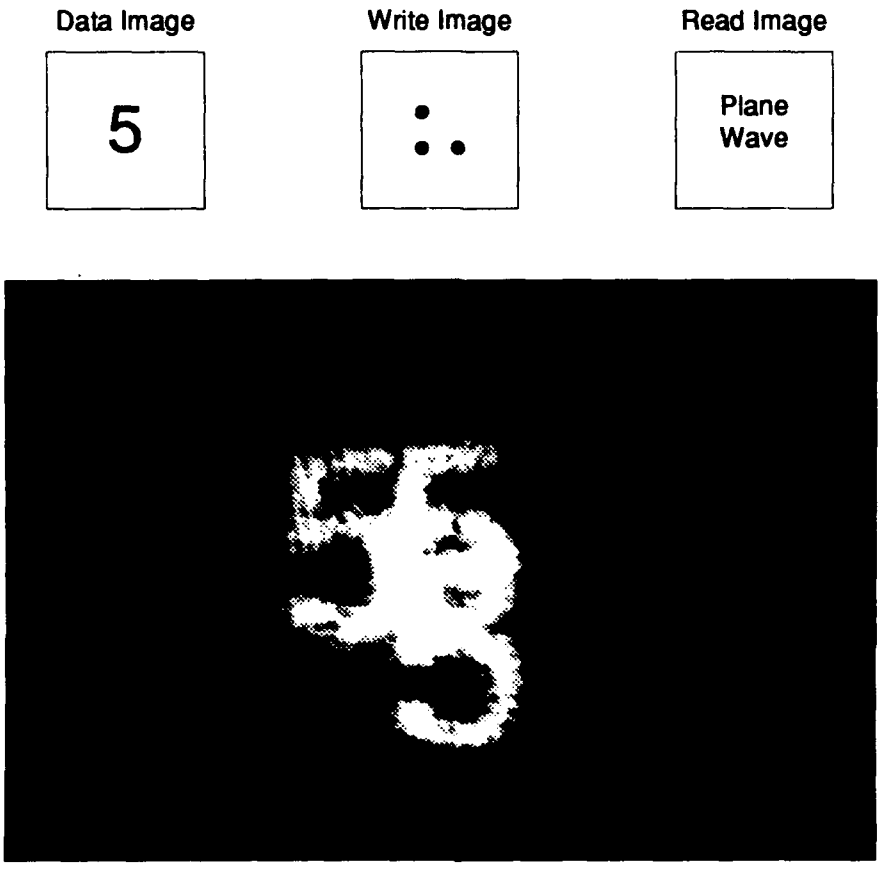

Figure 10. Echo image showing the correlation between a numeral "5" and three dots.

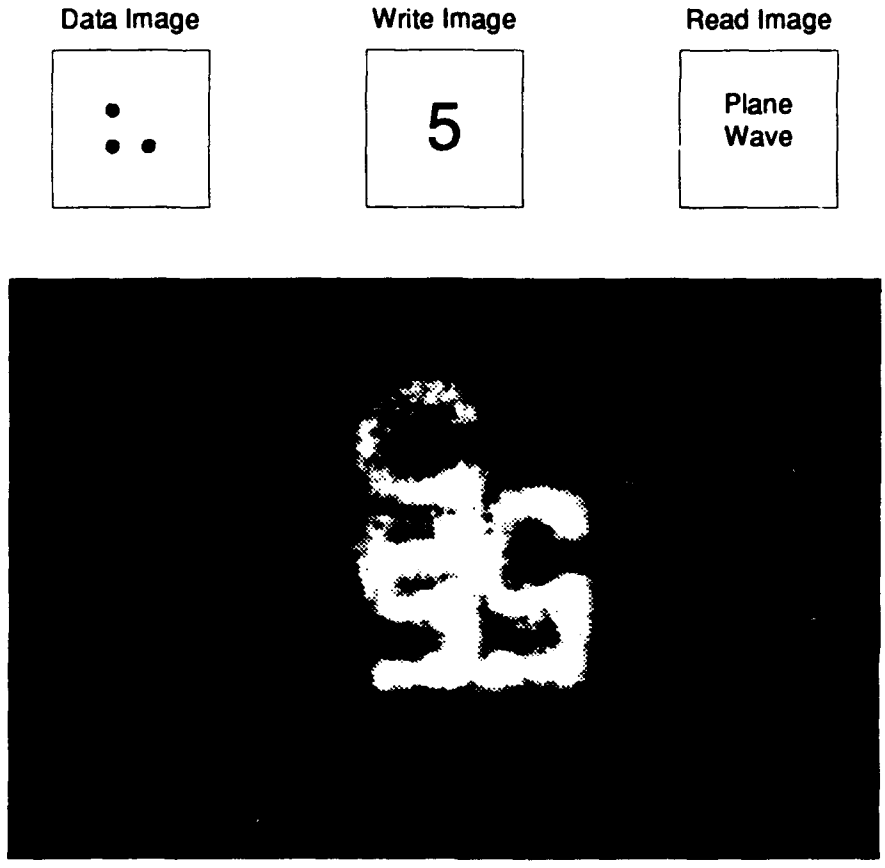

Figure 11. Echo image showing the correlation between three dots and a numeral "5".

The order of the input images has been changed (compare with that shown in Figure 10).

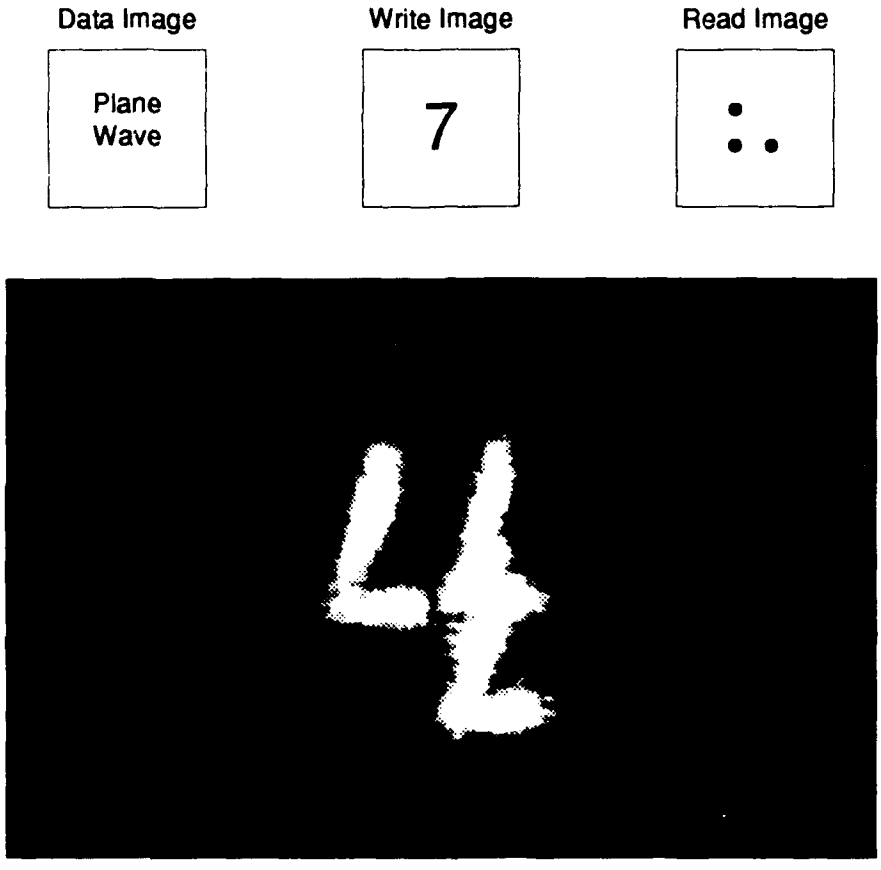

Figure 12. Echo image showing the convolution between a numeral "7" and three dots.

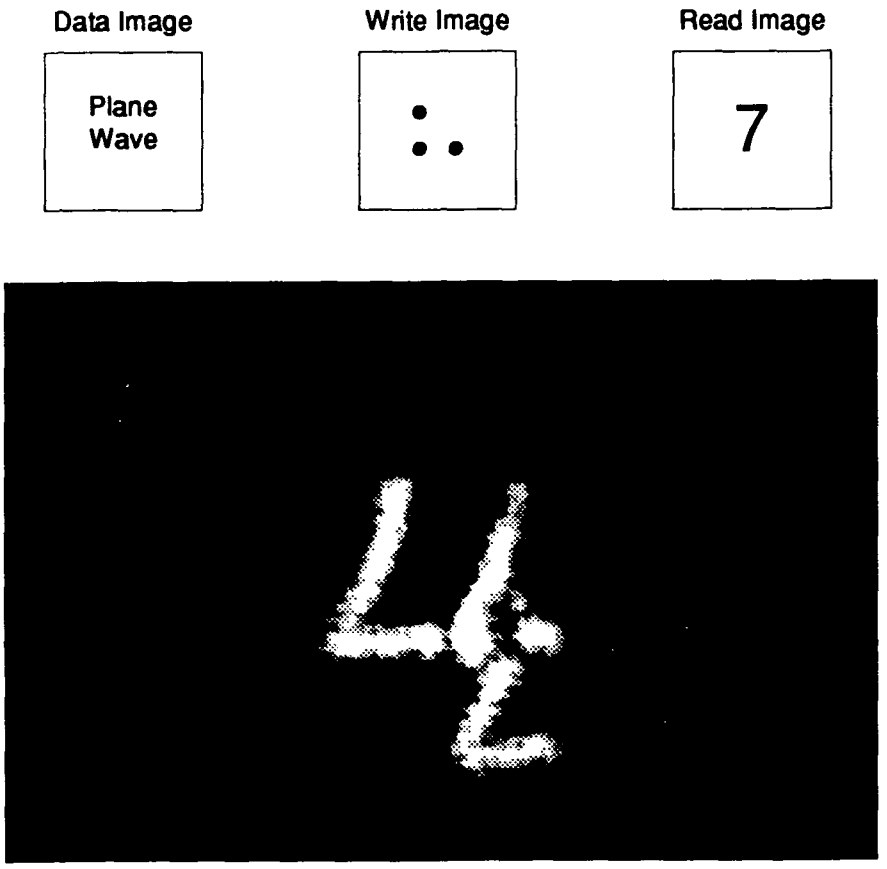

Figure 13. Echo image showing the convolution between a numeral "7" and three dots.
The order of the input data images has been changed (compare with that shown in Figure 12).

image, as shown in Figures 10 and 11, can also be expressed as a convolution of u_1 and u_2 (or u_3), except that only u_2 (or u_3) is inverted.

The above approach to image processing differs from conventional optical methods in several aspects. The most important one is its high speed, as has been demonstrated here. The operations were carried out on a nanosecond time scale, much faster than is possible with most other optical techniques, such as Van der Lugt holograms and four-wave mixing in photorefractive media.[18-22] Another advantage of this approach is that, because the processor itself is also an image storage device, thus one can store a large number of images and then correlate or convolute them with another image either immediately or after a short delay. This feature further increases the speed of the processor.

We should reemphasize that the above images were recorded from single echo pulses with the gated CCD camera, and no signal averaging was involved. The digitized pictures are of good quality.

HIGH-SPEED IMAGE PROCESSING

The above demonstrations of 2-D spatial correlation and convolution were limited to cases involving only two images at a time. As stated earlier, the stimulated echo is capable of simultaneously performing a large number of these operations. However, until now this ability had not been demonstrated experimentally. In the past, we have only shown the storage and retrieval of two images.[2] The quality of the retrieved images in the previous work was not good, and we were not able to comment on use of the stimulated echo for high-speed image processing. We have now demonstrated for the first time the multiple operations of two-image correlation using the stimulated echo technique.

The experimental setup for this work was very similar to the one shown in Figure 2, except that there were two second pulses here, each of which carried image information created with masks. The third pulse was again a plane wave. The time sequence in which the events occurred is shown in Figure 14, along with the wave vector (k_i) of each pulse, and the relative delays for each pulse were as follows: $t_{12} = 90$ ns, $t_{12'} = 110$ ns and $t_{2'3} = 15$ ns. The mask used for the first pulse was a numeral "7", while that for Pulse 2 (2') was two dots separated vertically (or horizontally), as shown in Figure 15. In recording the echo images, we used a 50-ns pulse to gate the image intensifier. We first chose an appropriate delay (say, τ_1) for the gate pulse so that only the first echo image was detected (see Figure 15b), which corresponds to the correlation between "7" and ":". After the delay was increased to $\tau_1 + 50$ ns, the second echo pulse was recorded (Figure 15c, correlation of "7" and ".."). Since the separation between the two

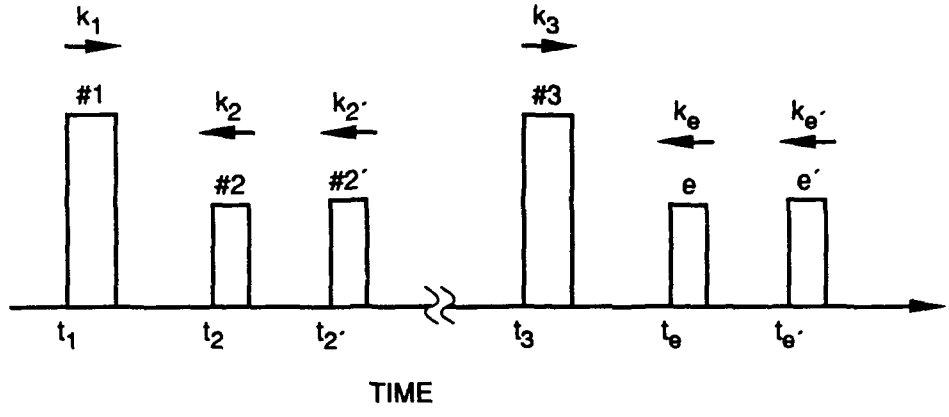

Figure 14. Temporal pulse sequence in the multiple write-pulse experiment.

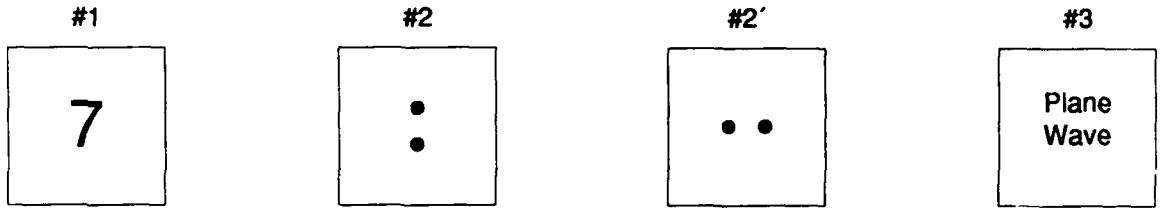

(a) Input images

(b) First echo image

(c) Second echo image

(d) Simultaneous recording of (b) and (c)

CP-1563-13

Figure 15. Input images and echo images retrieved in a high-speed image processing experiment.

echo pulses was 15 ns less than the gate width, both images could be recorded simultaneously with a delay of τ_1 + 20 ns, as shown in Figure 15d.

Figure 15 also shows no measurable crosstalk between the two retrieved images. This finding is important because it means that the correlation between two images can be performed at a much higher rate than was used in the work described in the previous section. In addition, the correlation provides a means for conducting high-speed pattern recognition which will be discussed.

In conclusion, we want to comment on possible improvements in the quality of the echo images, especially for the case of image processing. It is known that the Fourier spectrum of an image contains many high-frequency components that spread over the entire focal plane. These components are particularly important because they make a large contribution to the sharpness of the image. When an image is retrieved, one wants to collect as many of these components as possible to reconstruct a sharp echo image. This need effectively limits the size of the crystal as well as the angle between the laser beams to be used in the experiments. The sample must be large enough to collect most of the high-frequency components. In the case of two-image processing, it suggests using a coaxial geometry for the processor to meet the phase-matching condition in the entire focal plane, which means that the focal planes of the transform lenses must coincide with each other at the sample. Obviously, the latter requirement is not applicable to the case of image storage where only one lens is used. This dependence of echo image quality on the separation angle between the first and second pulses has been observed in our experiments.

HIGH-SPEED PATTERN RECOGNITION

In the last section, we discussed using the stimulated echo to perform two-image convolutions and correlations on a nanosecond time scale. We also showed that a number of these operations can be performed simultaneously by using multiple write pulses to further increase the processing speed. The results are very encouraging and provide a good basis for new applications, such as high-speed pattern recognition. Here we report on the extension of this work to pattern recognition.

Spatial correlation states that if two input images to be compared are identical, the resulting electric field (here the echo pulse) is simply a plane wave.[12] The reason is that one of the inputs is now a phase-conjugate replica of the other, and consequently the curvatures of the two incident beams cancel at the focal plane. With the arrangement shown in Figure 2, the resulting echo image at the outer focal plane of the transform lens will be simply a bright point. If the two input images are not the same, the echo pulse will differ from a plane wave and as a result, the echo image will not be a sharp point.

This approach to pattern recognition has been employed in our laboratory, and the results are shown in Figures 16 and 17. Here the pictures represent the echo images obtained from operations of correlation between two input images. Figure 16 shows the correlations between (a) two P's and (b) two R's. In both cases we obtained a bright point, which indicates high correlation between the input images.

Figure 17 shows a set of measurements designed to demonstrate the ability of the stimulated echo to identify characters by comparing a number of characters with a numeral "5". We started with two 5's, as shown in the top row of Figure 17. As expected, we detected a bright point, which suggests that the two images were highly correlated. When a numeral "7" was used as the data image, we obtained essentially no signal (second row in the figure). The same response was obtained for the letters R, Q, K, and J (the next four rows). However, when a "5" was reintroduced (bottom row), we again observed a bright spot.

Note that the only change in the experiment was the mask for the first (data) pulse. No other parameters, including the gain setting of the recording system, were changed during the experiment. Thus, with the same attenuation of signal required to obtain an unsaturated spot in the top and bottom rows (two 5's), we were not able to detect echo images in the cases of cross-correlation (the intervening rows) because the signal density was too low. The experimental

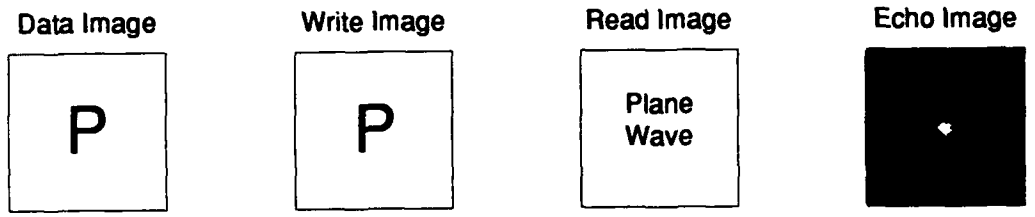

(a) Correlation between two P's

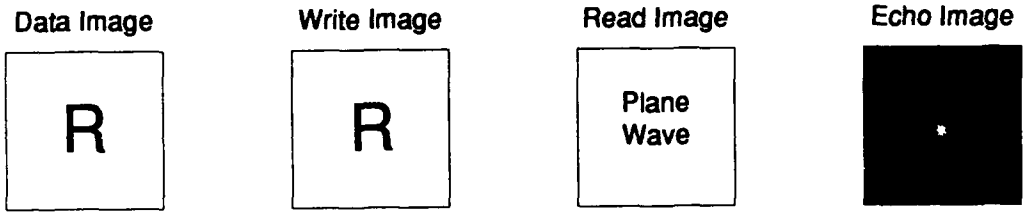

(b) Correlation between two R's

CP-1563-14

Figure 16. Echo images showing autocorrelations.

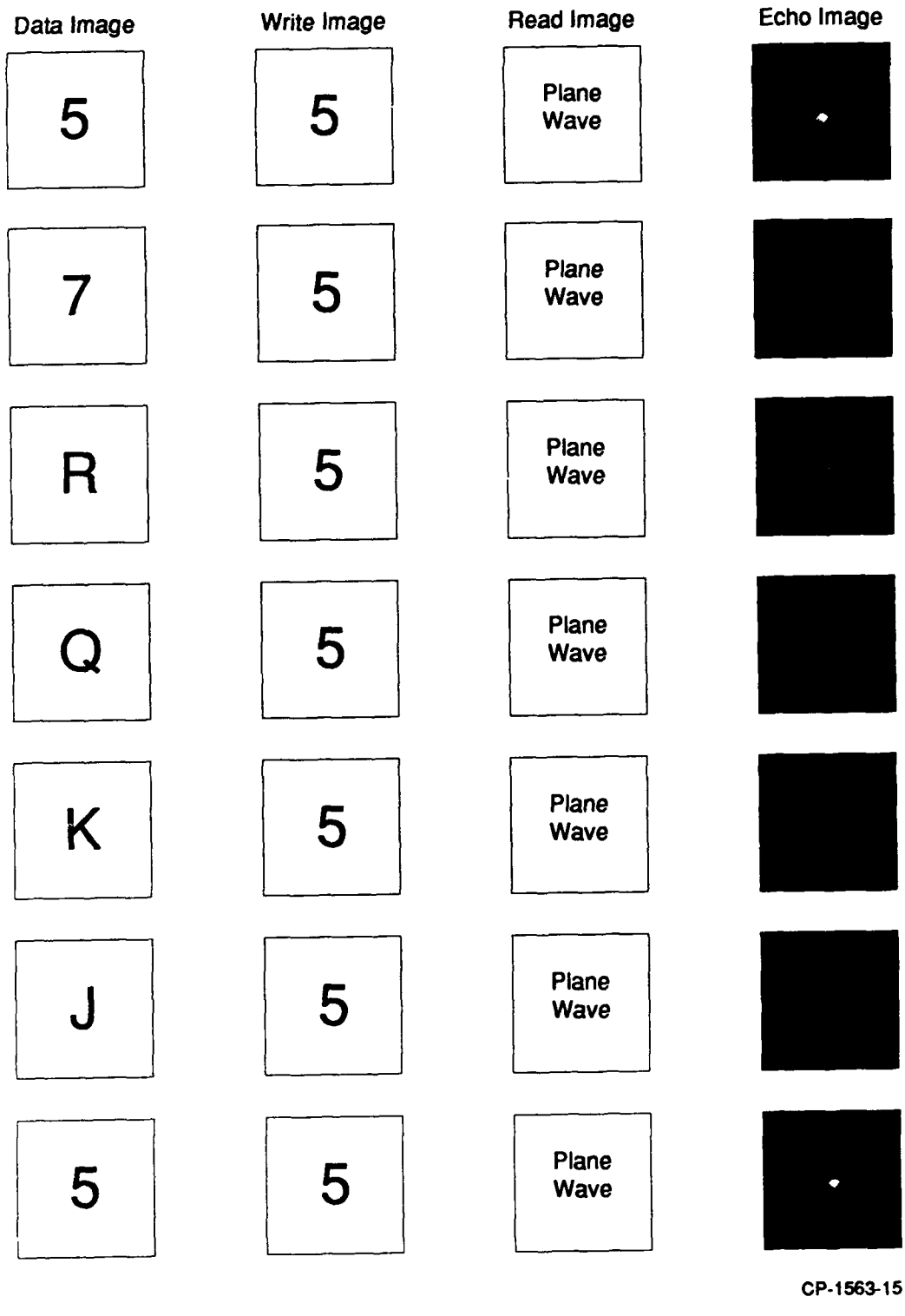

Figure 17. A set of correlation operations to demonstrate the potential of the stimulated echo technique for high-speed pattern recognition.

conditions used to obtain these measurements were identical to those used for two-image correlation (see Spatial Convolution and Correlation in the previous section).

These results represent the first experimental evidence that the stimulated echo can be used for pattern recognition. As has been demonstrated throughout this report, the technique has additional features that are not available with other methods for this type of application, such as high processing speed and the ability of storing a large number of images. These features are vital for a practical high-speed device for pattern recognition. For example, with the large storage capability, a large number of reference images can be stored as data pulses in the crystal by using a uniform write pulse. The information about an unknown image to be analyzed is carried by the read pulse. This arrangement will yield a large number of echo images, each of which will be the correlation between the unknown image and one of the reference images, similar to those shown in Figure 17. This approach will substantially increase the processing speed.

Although a number of issues must still be addressed—such as how to determine the degree of the correlation for precise identification of the image to be analyzed, what strategy should be used to analyze input images, and how to overcome problems like the technique's sensitivity to scale-size and orientation of the input images—we have successfully demonstrated the use of the stimulated echo for high-speed pattern recognition. The advantages of this technique over others in terms of its practical applications are clear. Currently, we are extending this work to the case of multiple data pulses to further increase the processing speed.

EFFECT OF TEMPERATURE ON ECHO INTENSITY

One of the most important aspects of our work on TDOM is to develop a better understanding of how various physical processes may affect the performance of the stimulated echo memory. One such consideration is the effect of temperature on the echo signal. Several mechanisms are believed to contribute to this temperature effect: direct phonon relaxation, the resonant two-phonon process, Raman relaxation, and the intrinsic Raman process.[23] These processes involving phonon relaxation in rare-earth solids lead to homogeneous broadening of spectral lines of rare-earth ions and hence reduce the dephasing time T_2 that determines the storage capacity of the echo memory. Thus, this parameter is critical in evaluating the performance of the TDOM. Below, we discuss our measurement of temperature-dependent echo intensity in Pr^{3+}:LaF_3.

The results presented here were obtained by measuring echo intensity as a function of temperature at a given t_{12} in Pr^{3+}:LaF_3. Although these results are not directly related to the dephasing time of the material, they can be compared with existing theoretical models to estimate its temperature dependence. To obtain the dephasing time directly, one must measure the echo intensity as a function of t_{12} at various temperatures. This approach requires the use of a cw dye laser to obtain variable delays, and this apparatus was not available at the time the measurement was made.

Figure 18 shows the measured echo intensity as a function of temperature for the $^3H_4$-$^3P_0$ transition in Pr^{3+}:LaF_3. The delays between pulses are t_{12}= 80 ns and t_{23}= 20 ns. The signal intensity remains constant at temperatures below 10 K and quenches rapidly above 10 K. This dependence is expected, since the echo intensity is related exponentially to $-1/T_2$.[24] To compare the echo intensity to theory, we employed a theoretical model developed by Yen et al.[11] for the $^3H_4$-$^3P_0$ transition in Pr^{3+}:LaF_3 and plotted it together with the measurement (Figure 18). The model takes into account all the phonon-induced processes mentioned above and, as shown in the figure, it agrees with the experimental results in general. However, one difference exists: the quenching temperature predicted by the model for t_{12}= 80 ns is approximately 4 kelvins below the measured temperature. This result is unexpected, because in applying the model we neglected other possible processes (such as spectral diffusion) that would further reduce the quenching temperature. Therefore, the measured temperature would be expected to be lower than the predicted one, in contrast to what is shown in Figure 18. One possible explanation for this discrepancy is that the model might not be appropriate for low temperatures because the model

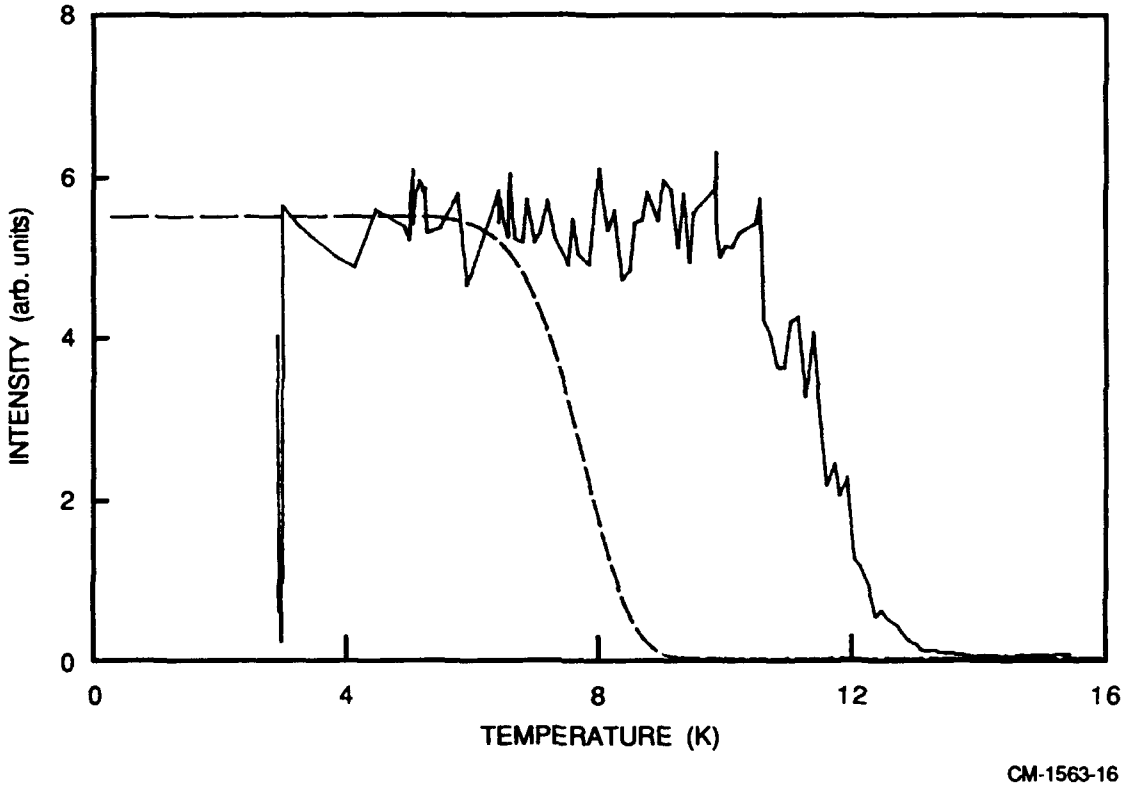

Figure 18. Temperature-dependent echo intensity.

The temporal difference between the first and second pulses is 80 ns. The dashed line is the theoretical prediction based on the model of Yen et al.[11]

parameters obtained by Yen et al. were based largely on experimental data above 77 K (only one data point is below 77 K, i.e., 4.2 K). In spite of this difference, both theory and experiment show that the echo signal diminishes rapidly once quenching takes place.

The above experimental results are useful because they provided information about the effect of temperature on the echo signal for the $^3H_4$-$^3P_0$ transition in Pr^{3+}:LaF_3 and allowed us to estimate its temperature-dependent dephasing time. However, as stated earlier, this measurement does not provide direct information about the dephasing time. A different and more direct approach is needed to obtain this information. We will pursue this work in the near future.

CONCLUSIONS AND FUTURE WORK

In the last year, we have examined the use of stimulated echoes for image storage and image processing. We have shown that the images retrieved from the stimulated echo memory are of high quality and high resolution. In addition, we demonstrated the use of this technique for simultaneously performing multiple two-image correlation operations and showed for the first time the extension of this work to high-speed pattern recognition. The results are very encouraging and demonstrate the potential for high-speed, high-density storage as well as high-speed image processing. This work was generally productive and successful and provided a good basis for further evaluation of TDOM.

The next step is to examine the use of TDOM for multiple-image storage and retrieval. This work will have important implications for high-speed image processing and pattern recognition and is currently under way. Additional effort is needed to further improve the quality and spatial resolution of the retrieved images; this work may include using a coaxial arrangement for the laser beams and increasing the laser beam cross section to collect high-frequency Fourier components. Finally, we will continue our efforts to investigate the various physical processes involved in the use of stimulated echoes for data storage and to obtain a good understanding of these processes for use in the future development of a high-performance, all-optics, data storage device.

REFERENCES

1. R. Kachru, SRI International Proposal No. PYU 90-311 to AFOSR (November 1990).
2. M. K. Kim and R. Kachru, Opt. Lett. **12**, 593 (1987).
3. E. Y. Xu, S. Kröll. D. L. Huestis, R. Kachru, and M. K. Kim, Opt. Lett. **15**, 562 (1990).
4. J. B. Morsink and D. A. Wiersma, in *Laser Spectroscopy* IV, H. Walther and K. W. Rothe, Eds. (Springer-Verlag, New York, 1979).
5. T. W. Mossberg, R. Kachru, S. R. Hartman, and A. M. Flusberg, Phys. Rev. A **20**, 1976 (1979).
6. M. Fujita, H. Nakasuka, H. Nakanishi, and M. Matsuoka, Phys. Rev. Lett. **42**, 974 (1979).
7. T. W. Mossberg, Opt. Lett. **7**, 77 (1982).
8. M. K. Kim and R. Kachru, Opt. Lett. **14**, 423 (1989).
9. M. K. Kim and R. Kachru, Appl. Opt. **28**, 2186 (1989).
10. Y. S. Bai, W. R. Babbitt, and T. W. Mossberg, Opt. Lett. **11**, 724 (1986).
11. W. M. Yen, W. C. Scott, and A. L. Schawlow, Phys. Rev. A **136**, 271 (1964).
12. J. W. Goodman, *Introduction to Fourier Optics* (McGraw Hill, New York, 1968).
13. I. McMichael, P. Yeh, and P. Bechwith, Opt. Lett. **12**, 507 (1987).
14. A. Yariv, Appl. Phys. Lett. **28**, 88 (1976).
15. G. J. Dunning and R. C. Lind, Opt. Lett. **7**, 558 (1982).
16. P. H. Beckwith, I. McMichael, and P. Yeh, Opt. Lett. **12**, 510 (1987).
17. D. M. Pepper, J. A. Yeung, D. Fekete, and A. Yariv, Opt. Lett. **3**, 7 (1978).
18. E. G. Paek and D. Pasltis, Opt. Eng. **26**, 428 (1987).
19. L.-S. Lee, M. M. Stoll, and M. C. Tackitt, Opt. Lett. **14**, 162 (1989).
20. J. L. Horner and J. R. Leger, Appl. Opt. **24**, 609 (1985).
21. D. Psaltis, E. G. Paek, and S. S. Verkatech, Opt. Eng. **23**, 698 (1984).
22. J. O. White and A. Yariv, Appl. Phys. Lett. **37**, 35 (1980).

23. G. F. Imbusch and R. Kopelman, in *Laser Spectroscopy of Solids*, W.M. Yen and P. M. Selzer, Eds. (Springer-Verlag, New York, 1981).

24. S. Kröll, E.Y. Xu, M. K. Kim, M. Mitsunaga, and R. Kachru, Phys. Rev. B. **41**, 11568 (1990).